Tropospheric products of the 2nd European GNSS reprocessing (1996-201

Jan Dousa, Pavel Vaclavovic, Michal Elias

NTIS - New Technologies for the Information Society, Geodetic Observatory Pecný, RIGTC
250 66 Zdiby, Czech Republic

Correspondence to: J. Douša (jan.dousa@pecny.cz)

Abstract

In this paper, we present results of the 2nd reprocessing of all data from 1996 to 2014 from all stations in the European GNSS permanent network as performed at the Geodetic Observatory Pecný (GOP). While the original goal of this research was to ultimately contribute to new realization of the European terrestrial reference system, we also aim to provide a new set of GNSS tropospheric parameter time series with possible applications to climate research. To achieve these goals, we improved a strategy to guarantee the continuity of these tropospheric parameters and we prepared several variants of troposphere modelling. We then assessed all solutions in terms of the repeatability of coordinates as an internal evaluation of applied models and strategies, and in terms of zenith tropospheric delays (ZTD) and horizontal gradients with those of ERA-Interim numerical weather model (NWM) reanalysis. When compared to the GOP Repro1 solution, the results of the GOP Repro2 yielded improvements of approximately 50% and 25% in the repeatability of the horizontal and vertical components, respectively, and of approximately 9% in tropospheric parameters. Vertical repeatability was reduced from 4.14 mm to 3.73 mm when using the VMF1 mapping function, a priori ZHD, and non-tidal atmospheric loading corrections from actual weather data. Raising the elevation cut-off angle from 3° to 7° and then to 10° increased RMS from coordinates' repeatability, which was then confirmed by independently comparing GNSS tropospheric parameters with the NWM reanalysis. The assessment of tropospheric horizontal gradients with respect to the ERA-Interim revealed a strong sensitivity of estimated gradients to the quality of GNSS antenna tracking performance. This impact was demonstrated at the Mallorca station, where gradients systematically grew up to 5 mm during the period between 2003 and 2008, before this behaviour disappeared when the antenna at the station was changed. The impact of processing variants on long-term ZTD trend estimates was assessed at 172 EUREF stations with time-series longer than 10 years, resulting in most significant impact, site-specific, due to the non-tidal atmospheric loading followed by the impact of changing elevation cut-off angle from 3° to 10°. The other processing strategy had very small or negligible impact on estimated trends.

Keywords: GPS, reprocessing, zenith tropospheric delay, tropospheric horizontal gradients, coordinate time series, reference frame

1 Introduction

The US Global Positioning System (GPS) became operational in 1995 as the first Global Navigation Satellite System (GNSS). Since that time, this technology has been transformed into a fundamental technique for positioning and navigation in everyday life. Hundreds of GPS permanent stations have been deployed for scientific purposes throughout Europe and the world, and the first stations have collected GPS data for approximately the last two decades. In 1994, a science-driven global network of continuously operating GPS stations was established by the International GNSS Service, IGS

(http://www.igs.org) of the International Association of Geodesy (IAG) to support the determination of precise GPS/GNSS orbits and, clocks and earth rotation parameters, which are necessary for obtaining high-accuracy GNSS analyses for scientific applications. A similar network, but regional in its scope, was also organized by the IAG Reference Frame Sub-Commission for Europe (EUREF) in 1996, which was called the EUREF Permanent Network (EPN), http://epncb.oma.be (Bruyninx et al. 2012). Although its primary purpose was to maintain the European Terrestrial Reference System (ETRS), the EPN also attempted to develop a pan-European infrastructure for scientific projects and co-operations (Ihde et al. 2014). Since 1996, the EPN has grown to include approximately 300 operating stations, which are regularly distributed throughout Europe and its surrounding areas. Today, EPN data are routinely analysed by 18 EUREF analysis centres.

Throughout the past two decades, GPS data analyses of both global and regional networks have been affected by various changes in processing strategy and updates of precise models and products, reference frames and software packages. To reduce discontinuities in products, particularly within coordinate time series, homogeneous reprocessing was initiated by the IGS and EUREF on a global and regional scale, respectively. To exploit the improvements in these IGS global products, the 2nd European reprocessing was performed in 2015-2016, with the ultimate goal of providing a newly realized ETRS.

Currently, station coordinate parameter time series from reprocessed solutions are mainly used in the solid earth sciences as well as to maintain global and regional terrestrial reference systems. Additionally, from an analytical perspective, the long-term series of estimated parameters and their residuals are useful for assessing the performances of applied models and strategies over a given period. Moreover, tropospheric parameters derived from this GNSS reanalysis could be useful for climate research (Yuan et al., 1993), due to their high temporal resolution and unrivalled relative accuracy for sensing water vapour when compared to other techniques, such as radio sounding, water vapour radiometers, and radio occultation (Ning, 2012). In this context, the GNSS Zenith Tropospheric Delay (ZTD) represents a site-specific parameter characterizing the total signal path delay in the zenith due to both dry (hydrostatic) and wet contributions of the neutral atmosphere, the latter of which is known to be proportional to precipitable water (Bevis et al. 1994).

With the 2nd EUREF reprocessing, the secondary goal of the GOP was to support the activity of Working Group 3 of the COST Action ES1206 (http://gnss4swec.knmi.nl), which addresses the evaluation of existing and future GNSS tropospheric products, and assesses their potential uses in climate research. For this purpose, GOP provided several solution variants, with a special focus on optimal tropospheric estimates, including VMF1 vs. GMF mapping functions, the use of different elevation cut-off angles, and estimates of tropospheric horizontal gradients using different time resolutions. Additionally, in order to enhance tropospheric outputs, we improved the processing strategy in a variety of ways compared to the GOP Repro1 solutions (Douša and Václavovic, 2012): 1) by combining tropospheric parameters in midnights and across GPS week breaks, 2) by checking weekly coordinates before their substitutions in order to estimate tropospheric parameters, and 3) by filtering out problematic stations by checking the consistency of daily coordinates. The results of this GOP reprocessing, including all available variants, were assessed using internal evaluations of applied models and strategy settings, and external validations with independent tropospheric parameters derived from numerical weather reanalyses.

The processing strategy used in the 2nd GOP reanalysis of the EUREF permanent network is described in Section 2 and, new approach that is developed to guarantee a continuity of estimated tropospheric parameters at midnights as well as between different GPS weeks is summarised in Section 3. The relationship between mean tropospheric horizontal gradients and the quality of low-elevation GNSS tracking is explained in Section 4. The results of internal and external evaluations of GOP solution variants and processing models are presented in Section 4 and, the assessment of impacts of specific variants on estimated ZTD trends in Section 5. The last section concludes our findings and suggests avenues of future research.

2 GOP processing strategy and solution variants

The EUREF GOP analysis centre was established in 1997, and contributed to operational EUREF analyses until 2013 by providing final, rapid, and near real-time solutions. Recently, GOP changed its contributions to that of a long-term homogeneous reprocessing of all data from the EPN historical archive. The GOP solution of the 1st EUREF reanalysis (Repro1) (Völksen, 2011) comprised the processing of a sub-network of 70 EPN stations during the period of 1996-2008. In 2011, for the first time, GOP reprocessed the entire EPN network (spanning a period of 1996-2010) in order to validate the European reference frame and to provide the first homogeneous time series of tropospheric parameters for all EPN stations (Douša and Václavovic, 2012).

In the 2nd EUREF reprocessing (Repro2), GOP analysed data obtained from the entire EPN network from a period of 1996-2014 using the Bernese GNSS Software V5.2 (Dach et al., 2015). The GOP strategy relies on a network approach utilizing double-difference observations. Only GPS data from the EPN stations were included according to official validity intervals provided by the EPN central Bureau (http://epncb.oma.be). Two products were derived from the reprocessing campaign in order to contribute to a combination at the EUREF level performed by the coordinator of analysis centres and the coordinator of troposphere products: 1) site coordinates and corresponding variance-covariance information in daily and weekly SINEX files and 2) site tropospheric parameters in daily Tro-SINEX files.

This GOP processing was clustered into eight subnetworks (Figure 1) and then stacked into daily network solutions with pre-eliminated integer phase ambiguities when ensuring strong ties to IGS08 reference frame. This strategy introduced state-of-the-art models (IERS Conventions, 2010) that are recommended as standards for highly accurate GNSS analyses, particularly for the maintenance of the reference frame. Additionally, the use of precise orbits obtained from the 2nd CODE global reprocessing (Dach et al., 2014) guaranteed complete consistency between all models on both the provider and user sides. Characteristics of this GOP data reprocessing strategy and their models are summarized in Table 1. Additionally, seven processing variants were performed during the GOP Repro2 analysis for studying selected models or settings: a) applying tropospheric mapping function model GMF (Böhm et al., 2006a) vs. VMF1 (Böhm et al., 2006b), the latter based on actual weather information, b) increasing the temporal resolution of tropospheric linear horizontal gradients in the north and east directions, c) using different elevation cut-off angles, d) modelling atmospheric loading effects, and e) modelling higher-order ionospheric effects. Table 2 summarizes the settings and models of solution variants selected for generating coordinate and troposphere products, which are supplemented with variant rationales.

Within the processing, we screened station coordinate repeatabilities from weekly combined solutions and we identified any problematic station for which north/east/up residuals exceeded 15/15/30 mm or RMS of north/east/up coordinate component exceeded values 10/10/20 mm. Such station was a priori excluded from the tropospheric product for the corresponding day. There were other standard control procedures within the processing when individual station could have been excluded, e.g. if a) less than 60% of GNSS data available, b) code or phase data revealed poor quality, c) station metadata were found inconsistent with data file header information (receiver, antenna and dome names, antenna eccentricities) and, d) phase residuals were too large for all satellites in the processing period indicating a problem with station. Tropospheric parameters were estimated practically without constrains (a priori sigma greater than 1 m) thus parameter formal errors reflect relative uncertainties of estimates. Usually, large errors indicate the lack of observations contributing to the parameter. During the tropoposheric parameter evaluations, we applied filter for exceeding formal errors of estimated parameters (ZTD sigma greater than 3 mm, normal cases stay below 1 mm).

3 Ensuring ZTD continuity at midnights

When site tropospheric parameter time series generated from the 2nd EUREF reprocessing are applied to climate research, they should be free of artificial offsets in order to avoid misinterpretations (Bock et al., 2014). However, GNSS processing is commonly performed on a daily basis according to adopted standards for data and product dissemination. Thus far, EUREF analysis centres have provided independent daily solutions, although precise IGS products are combined and distributed on a weekly basis. Station coordinates are estimated on a daily basis and are later combined to form more stable weekly solutions. According to the EUREF analysis centre guidelines (http://www.epncb.oma.be/_documentation/guidelines/guidelines_analysis_centres.pdf), weekly coordinates should be used to estimate tropospheric parameters on a daily basis, but there are no requirements with which to guarantee the continuity of tropospheric parameters at midnights. Additionally, there are also discontinuities on a weekly basis, as neither daily coordinates nor hourly tropospheric parameters are combined across midnights between corresponding adjacent GPS weeks.

The impact of a 3-day combination was previously studied when assessing the tropospheric parameters stemming from the 2nd IGS reprocessing campaign 2016 in the GOP-TropDB (Győri and Douša, 2016). We compared two global tropospheric products provided by the analysis centre CODE (Centre of Orbit Determination in Europe) differing only in the procedure of combining tropospheric parameters from the daily original solutions. The first product, COF, was based purely on a single-day solution while the second product, COD, on a 3-day combination (Dach et al., 2014). A sub-daily statistics were calculated by comparing 2-hour ZTD estimates from both products during 2013. There were no significant biases observed, but mean standard deviation estimated from differences reached 0.8 mm in ZTD over a day, but almost 1.8 mm close to the day boundaries. Similarly, a dispersion characterized by 1-sigma over all stations reached 0.5 mm for the former, but up to 1.2 mm for the latter. Actual differences in ZTDs could even be significantly larger reaching up to several millimetres or more as the middle values of 2-hour ZTD estimates could have been compared only, i.e. at 1:00 UTC and 23:00 UTC.

During the 1st GOP reprocessing, there was no way to guarantee tropospheric parameter continuity at midnight, as the troposphere was modelled by applying a piecewise constant model. In these cases, tropospheric parameters with a temporal resolution of one hour were reported in the middle of the

hour, as was originally estimated. In the 2nd GOP reprocessing, using again hourly estimates, we applied a piecewise linear model for the tropospheric parameters. The parameter continuities at midnights were not guaranteed implicitly, but only by an explicit combination of parameters at daily boundaries. For the combination procedure we used three consecutive days while the tropospheric product stems from the middle day. The procedure is done again for three consecutive days shifted by one day. A similar procedure, using the piecewise constant model, was applied for estimating weekly coordinates which aimed to minimize remaining effects in consistency at transition of GPS weeks (at Saturday midnight). The coordinates of the weekly solution corresponding to the middle day of a three-day combination were fixed for the tropospheric parameter estimates. In the last step, we transformed the piecewise linear model to the piecewise constant model expressed in the middle of each hourly interval (HR:30), which was saved in the TRO-SINEX format to support the EUREF combination procedure requiring such sampling. The original piecewise linear parameter model was thus lost and to retain this information in the official product in the TRO-SINEX format, we additionally stored values for full hours (HR:00). Figure 2 summarizes four plots displaying tropospheric solutions with discontinuities in the left panels (a), (c) and enforcing tropospheric continuities in the right panels (b, d). While the upper plots (a), (b) display the piecewise constant model, bottom plots (c), (d) indicates the solution representing the piecewise linear model. The GOP Repro1 implementation is thus represented by Figure 2(a) plot while the GOP Repro2 solution corresponds to Figure 2(d) and, alternatively Figure 2(b).

These theoretical concepts were practically tested using a limited data set in 1996 (Figure 3). The panels in Figure 3 follow the organization of the theoretical plots shown in Figure 2; corresponding formal errors are also plotted along with estimated ZTDs. Discontinuities are visible in the left-hand plots and are usually accompanied by increasing formal errors for parameters close to data interval boundaries. As expected, discontinuities disappear in the right-hand plots. Although the values between 23:30 and 00:30 on two adjacent days are not connected by a line in the top-right plot, continuity was enforced for midnight parameters anyway, as seen in the bottom-right plot. Formal errors also became smooth near day boundaries, thus characterizing the contribution of data from both days and demonstrating that the concept behaves as expected in its practical implementation.

4 Quality of the observations and impact on tropospheric gradients

Recently, we have developed a new interactive web interface to conduct tropospheric parameter comparisons in the GOP-TropDB (Győri and Douša, 2016), which is being prepared for the IGS Tropospheric Working Group web (http://twg.igs.org/). Using the interface, we observed large systematic tropospheric gradients during specific years at several EPN stations. Generally, from GNSS data, we can only estimate total tropospheric horizontal gradients without being able to distinguish between dry and wet contributions. The former is mostly due to horizontal asymmetry in atmospheric pressure, and the latter is due to asymmetry in the water vapour content. The latter is thus more variable in time and space than the former (Li et al., 2015). Regardless, mean gradients should be close to zero, whereas dry gradients may tend to point slightly more to the equator, corresponding to latitudinal changes in atmosphere thickness (Meindl et al., 2004). Similarly, orography-triggered horizontal gradients can appear due to the presence of high mountain ranges in the vicinity of the station (Morel et al., 2015). Such systematic effects can reach the maximum sub-millimetre level, while a higher long-term gradient (i.e. that above 1 mm), is likely more indicative of issues with site

instrumentation, the environment, or modelling effects. Therefore, in order to clearly identify these systematic effects, we also compared our gradients with those calculated from the ERA-Interim.

It is beyond the scope of this paper to investigate in detail the correlation between tropospheric horizontal gradients and effects such as, for example, antenna tracking performance. However, we do observe a strong impact in the most extreme case identified when comparing gradients from the GNSS and the ERA-Interim for all EPN stations. Figure 4 shows the monthly means of differences in the north and east tropospheric gradients from the MALL station (Mallorca, Spain). These differences increase from 0 mm up to -4 mm and 2 mm for the east and north gradients, respectively, within the period of 2003/06 - 2008/10. Such large monthly differences in GNSS and NWM gradients are not realistic, and were attributed to data processing when long-term increasing biases dropped down to zero on November 1, 2008, immediately after the antenna and receiver were changed at the station. During the same period, also yearly mean ZTD differences to ERA-Interim steadily changed from about 3 mm to about -12 mm and immediately dropping down to -2 mm in 2008 after the antenna change.

The EPN Central Bureau (http://epncb.oma.be), operating at the Royal Observatory of Belgium (ROB), provides a web service for monitoring GNSS data quality and includes monthly snapshots of the tracking characteristics of all stations. The sequence of plots displayed in Figure 5, representing the interval of interest (2002, 2004, 2006 and 2008), reveals a slow but systematic and horizontally asymmetric degradation of the capability of the antenna to track low-elevation observations at the station. Therefore, we analysed days of the year (DoY) 302 and 306 (corresponding to October 28 and November 1, 2008) with the in-house G-Nut/Anubis software (Václavovic and Douša, 2016) and observed differences in the sky plots of these two days. The left-hand plot in Figure 6 depicts the severe loss of dual-frequency observations up to a 25° elevation cut-off angle in the South-East direction (with an azimuth of 90°-180°), which cause the tropospheric linear gradient of approximately 5 mm to point in the opposite direction. Figure 10 also demonstrates that an increasing loss of second frequency observations appears to occur in the East (represented as black dots). The right-hand plot in this figure demonstrates that both of these effects fully disappeared after the antenna was replaced on October 30, 2008 (DoY 304), resulting in the appearance of normal sky plot characteristics and a GLONASS constellation with one satellite providing only single frequency observations (represented as black lines).

This situation demonstrates the high sensitivity of the estimated gradients on data asymmetry, particularly at low-elevation angles. The systematic behaviour of these monthly mean gradients, their variations from independent data and a profound progress over time, seem to be useful indicators of instrumentation-related issues at permanent GNSS stations. It is also considered that gradient parameters can be valuable method as a part of ZTD data screening procedure (Bock et al., 2016).

Although the station MALL represented an extreme case, biases at other stations were observed too, e.g. GOPE (1996-2002), TRAB (1999-2008), CREU (2000-2002), HERS (1999-2001), GAIA (2008-2014) and others. Site-specific, spatially or temporally correlated biases suggest different possible reasons such as site-instrumentation effects including the tracking quality and phase centre variation models, site-environment effects including multipath and seasonal variation (e.g. winter snow/ice coverage), edge-network effects when processing double-difference observations, spatially correlated effects in reference frame realization and possibly others. The problematic stations and periods mentioned

above were however still included in comparisons and trend analysis because of the lack of objective criteria for their identification, which should be studied in future.

5 Assessment of reprocessing solutions

GOP variants and reprocessing models were assessed by a number of criteria, including those of the internal evaluations of repeatability of station coordinates, residuals at reference stations, and the external validation of ZTDs and tropospheric horizontal gradients with data from numerical weather model (NWM) reanalyses.

5.1 Repeatability of station coordinates

We used coordinate repeatability to assess the quality of models applied in GNSS analysis. To be as thorough as possible, we not only assessed all GOP Repro2 variants but also assessed two GOP Repro1 solutions in order to discern improvements within the new reanalyses. The two Repro1 solutions differed in their used reference frames and PCV models: IGS05 and IGS08.

Table 3 summarizes mean coordinate repeatability in the north, east and up components of all stations from their weekly combinations. All GOP Repro2 solution variants reached approximately 50% and 25% of the lower mean RMS of coordinate repeatability when compared to the GOP Repro1/IGS08 solution in its horizontal and vertical components, respectively. These values represent even greater improvements when compared to the GOP-Repro1/IGS05 solution. Comparing these two Repro1 solutions clearly demonstrates the beneficial impact of the new PCV models and reference frames. The observed differences between Repro2 and Repro1 also indicate an overall improvement of the processing software from V5.0 to V5.2, and the enhanced quality of global precise orbit and earth orientation products.

Various GOP Repro2 solutions were also used to assess the selected models. Variants GO0 and GO1 differ in their mapping functions (GMF vs VMF1) used to project ZTDs into slant path delays. These comparisons demonstrate that vertical component repeatability improved from 4.14 mm to 3.97 mm, whereas horizontal component repeatability decreased slightly. By increasing the elevation cut-off angle from 3° to 7° (GO2) and 10° (GO3), we observed a slight increase in RMS from repeatability of all coordinates. This can be explained by the positive impact of low-elevation observations on the decorrelation of height and tropospheric parameters, despite the fact that applied models (such as elevation-dependent weighting, PCVs, multipath) are still not optimal for including observations at very low elevation angles. On the other hand, it should be noted that the VMF1 mapping function is particularly tuned to observations at 3° elevation angle which leads to biases at higher elevation angles, Zus et al. (2015).

The GO4 solution represents an official GOP contribution to EUREF combined products. It is identical to the variant GO1, but applies a non-tidal atmospheric loading. Steigenberger et al. (2009) discussed the importance of applying non-tidal atmospheric loading corrections together with precise a priori ZHD model. It has been concluded that using mean, or slowly varying, empirical pressure values for estimating a priori ZHD instead of true pressure values results in a partial compensation of atmospheric loading effects which is the case of GO1 solution. A positive 10% improvement in height repeatability was observed for the GO4 solution. Our improvement was slightly lower than in a global scope reported by Dach et al. (2011) with an improvement of 10-20% over all stations. As the effect depends

on selected stations, a slightly higher impact in a global scale might be attributed to the station distribution, particularly differences in term of latitude and altitude.

No impact was observed from the higher-order ionospheric effects (GO4 vs. GO5) in term of coordinate repeatability. As the effect is systematic within the regional network (Fritsche et al., 2005) and it was mostly eliminated by using reference stations in the domains of interest. The combination of tropospheric horizontal gradients from 6-h to 24-h time resolution (GO4 vs. GO6), using the piecewise linear model, had a negligible impact on the repeatability of station coordinates too.

5.2 Reference frame - residuals at fiducial stations

The terrestrial reference frame (Altamimi et al., 2001) is a realization of a geocentric system of coordinates used by space geodetic techniques. To avoid a degradation of GNSS products, differential GNSS analysis methods require a proper referencing of the solution to the system applied in the generation of precise GNSS orbit products. For this purpose, we often use the concept of fiducial stations with precise coordinates well-known in the requested system. Such stations are used to define the geodetic datum while their actual position can be re-adjusted by applying a condition minimizing coordinate residuals. None station is able to guarantee a stable monumentation and unchanged instrumentation during the whole reprocessing period. Thus a set of about 50 stations, with 100 and more time periods for reference coordinates, was carefully prepared for datum definition in the GOP reprocessing. An iterative procedure was applied then for every day by comparing a priori reference coordinates with actually estimated ones and excluding fiducial station exceeding differences by 5, 5 and 15 mm in north, east and up components.

Figure 7 shows the evolution of the number of actually used fiducial stations (represented as red dots) from all configured fiducial sites (represented as black dots) after applying an iterative procedure of validation on a daily basis. This reprocessing began with the use of 16-20 fiducial stations in 1996, and this number increased to reach a maximum of over 50 during the period from 2003-2011. After 2011, this number decreased, due to a common loss of reference stations available from the last realization of the global terrestrial reference frame without changes in its instrumentation. In most cases, only 2 or 3 stations were excluded from the total number, however, this number is lower for some daily solutions, indicating the removal of even more stations. The lowest number of fiducial sites (12) was identified on day 209 of the year 1999 while, but low numbers were, generally, observed at the beginning of the reprocessing period, in 1996. We observed consistent mean RMS errors for horizontal, vertical, and total residuals of 6.47, 10.22, and 12.25 mm and 4.83, 7.94, 9.35 mm for daily and weekly solutions, respectively, which demonstrate the stability of the reference system in the reprocessing. The seasonality in height coordinate estimates characterized by the RMS of residuals from the reference frame realization is dominated by errors due to modelling of the troposphere. We believe, the main contribution stems from the insufficiencies in modelling of wet tropospheric delay, as the effect has the most pronounced seasonal signal within the GNSS data analysis. Additionally, the estimated station ZTD parameters and height are difficult to de-correlate. In the next section, the strong seasonal variation in comparing zenith total delays estimated from GNSS and NWM data is clearly visible.

5.3 Zenith total delays

We compared all reprocessed tropospheric parameters with respect to independent data from the ERA-Interim global reanalysis (Dee et al. 2011) provided by the European Centre for Medium-Range

Weather Forecasts (ECMWF) from 1969 to the present. For the period of 1996-2014, we calculated tropospheric parameters (namely ZTD and tropospheric horizontal linear gradients) from the NWM for all EPN stations using the GFZ (German Research Centre for Geosciences) ray-tracing software (Zus et al., 2014). The comparison of tropospheric parameters was performed by applying the linear interpolation of GNSS parameters to the original NWM 6-hour representation, using the GOP TropoDB (Győri and Douša, 2016). For monthly statistics discussed in this section, we applied an iterative procedure for outlier detection using the 3-sigma criteria calculated from the compared differences.

Table 4 summarizes comparisons of GNSS ZTDs, and tropospheric horizontal gradients, from all GOP processing variants with those obtained from the ERA-Interim. Mean biases and standard deviations were first calculated for each stations and each month and then mean and standard deviation of these values were computed, characterizing dispersions of all statistical values over the ensemble of stations.

The results in the table indicate a mean ZTD bias -1.8 mm for all comparisons (GNSS – NWM) suggesting ZTDs achieved from the NWM reanalysis are drier than those obtained from GNSS reprocessing. Similar biases have been observed for all other European GNSS re-processing products during the period of 1996-2014 (Pacione et al., 2017). On the other hand, when processing the ERA-Interim using two different software and methodologies within the GNSS4SWEC Benchmark campaign (Dousa et al., 2016) during May and June of 2013 in Central Europe, and by their comparing to two GNSS reference products based on different processing methods, we observed bias differences within ±0.4 mm in ZTD. As neither GNSS nor NWM is able to sense the troposphere with an absolute accuracy better than the bias that we observed, we cannot make any conclusion, but its independence of the GNSS software. A mixture of common processing aspects such as ~~scope~~ of GNSS network, applied tropospheric model, precise orbit product and others could still cause such a small biases in GNSS analysis at least.

Comparing the results of the official GOP Repro2 solution (GO4) to those of the legacy solution (GO0) demonstrates an overall improvement of 9%, which corresponds to a similar comparison between the EUREF Repro1 and Repro2 products (Pacione et al., 2017). The improvement is assumed to be even larger (indicated by the coordinate repeatability), ~~as the quality of ZTD retrievals are generally lower for NWM compared to GNSS from various intra-/inter-technique comparisons~~ (Douša et al., 2016, Kačmařík et al., 2017, Bock and Nuret, 2009).

Comparing the GO1 and GO0 variants demonstrates that the VMF1 mapping function outperforms GMF in term of standard deviation if the elevation cut-off angle of 3° is used. The change of mapping function together with the use of more accurate a priori ZHD, resulted in the ZTD standard deviation improving from 8.8 mm (GO0) to 8.3 mm (GO1). However, bias was slightly increased which could be partly attributed to the use of mean pressure model for a priori ZHD calculation and compensating part of the non-tidal atmospheric loading (see Section 5.1). Using non-tidal atmospheric loading corrections along with precise modelling of a priori ZHD contributed to a small reduction of the bias from -2.0 mm to -1.8 mm and, mainly, to the improvement by reducing this ZTD accuracy to 8.1 mm (GO4). This corresponds with the previous assessment of the repeatability of station coordinates. Degradation in ZTD precision was also observed when the elevation cut-off angle was raised from 3° to 7° (GO2) or 10° (GO3). No impacts on ZTD were, however, visible neither from additional modelling of high-order ionospheric effects (GO5) nor from stacking of 6-hour horizontal gradients into daily piecewise linear estimates (GO6).

Figure 8 displays the time series of statistics from comparisons of the GOP official ZTD product (GO4) with respect to the results of the ERA-Interim reanalysis. Mean bias and standard deviation were derived from the monthly statistics of the 6-hourly GNSS-ERA differences. A 1-sigma range of the mean values, represented by error bars, are additionally derived from all stations on a monthly basis. Although the time series show homogeneous results over the given time span, a small increase in the mean standard deviation over time likely corresponds with increasing number of EPN sites, rising from approximately 30 to 300. The early years (1996-2001) also display a worse overall agreement in 1-sigma range of mean values over all stations, which can be attributed to the varying quality of historical observations and precise orbit products. The mean bias varies from –3 to 1 mm during the period of 1996-2014, with a long-term mean of -1.8 mm (Table 4). The long-term mean is also relatively small compared to the ZTD mean 1-sigma range of 3-5 mm.

5.4 Tropospheric horizontal linear gradients

Additional GNSS signal delay due to the tropospheric gradients were developed by McMillan (1995). The complete tropospheric model for the line-of-sight delay (ΔD_T) using parameters zenith hydrostatic delay (ZHD), zenith wet delay (ZWD) and first-order horizontal tropospheric gradients G_N and G_E, all expressed in units of length, is described as follows

$$\Delta D_T = mf_h(e)ZHD + mf_w(e)ZWD + mf_g(e)\cot(e)[G_N\cos(A) + G_E\sin(A)] \quad (1)$$

where *e* and *a* are observation elevation and azimuth angles and mf_h, mf_w, mf_g are hydrostatic, wet and gradient mapping functions representing the projection from an elevation to the zenith. Horizontal gradients should optimally represent a ZTD change in a distances for north and east directions as it could be represented by terms $G_N\cot(e)$ and $G_E\cot(e)$ in the equation. However, the gradients need to be parametrized practically with respect to observation elevation angle instead of the distance theoretically applicable to the tropospheric effect at various elevation angles. The interpretation of the tropospheric horizontal gradients in the Bernese software represents north and east components of angle applied for the tilting the zenith direction in the mapping function with gradients representing (in unit of length) the tilting angle multiplied by the delay in zenith (Meindl et al., 2004).

Similarly as in case of ZTD and coordinate assessment, Table 4 shows that tropospheric gradients became worse when raising the elevation cut-off angle from 3° to 7° (GO2) or 10° (GO3). Mean standard deviations of the GO2 and GO3 solutions increased by 8% and 12%, respectively, which is valid for the whole period of monthly time series (not showed). No significant differences in temporal variations of mean biases of the north and east tropospheric gradients variants were identified while they shared a higher variability during the years 1996-2001. No impact of modelling of high-order ionospheric effects (GO5) was observed. Statistics of GO4 and GO6 solutions compared to ERA-Interim revealed that standard deviations dropped from 0.38 mm to 0.28 mm and from 0.40 mm to 0.29 mm for the east and north gradients, respectively. Worse performance of the GO4 solution is attributed to the fact that tropospheric horizontal gradients were estimated with a 6-h sampling interval using the piecewise linear model with applying practically no absolute or relative constraints. In such cases, increased correlations of the gradients with other parameters can cause instabilities in processing certain stations at specific times; the gradients absorb some remaining errors in the GNSS analysis model. The mean biases of the tropospheric gradients are considered to be negligible, but it was

demonstrated in Section 4 that some large systematic effects were indeed discovered and attributed to the quality of GNSS signal tracking.

Figure 9 displays monthly time series of statistics from comparisons of the GNSS and NWM tropospheric horizontal gradients in north and east directions. Two solutions are highlighted in order to demonstrate the impact of different parameter temporal resolutions; a 6-hour resolution is used for GO4 and a 24-hour resolution is used for GO6. Seasonal variations are mainly pronounced when observing mean standard deviations (top plot), whereas gradual improvement is more pronounced for mean biases (bottom plot). The reduction of the initial mean biases in horizontal gradients, and the corresponding 1-sigma ranges over the values from the ensemble of stations, can be attributed to the improved availability and quality of low elevation observation tracking. Elevation cut-off angles for collecting GNSS observations were initially configured station by station, ranging from 0° to 15°, until 2008 when the elevation cut-off angle 0° was recommended for all the stations.

Mean standard deviations and their 1-sigma ranges over all stations (Figure 9, top plot) are lower by a factor of 1.3 for the solution with 24-hour resolution (GO6) compared to the 6-hour resolution (GO4); the impact is also pronounced especially in the early years of the dataset. The improvement factor ranges from 1.03 to 1.65 with the mean value of 1.35 overall stations and it is usually higher for years before 2001. Theoretically, with 4 times more observations in GO6 the standard deviation was expected to be divided by a factor of 2. This discrepancy indicates serious correlations in errors which are among others stemming from the errors in precise products and models. Significant improvements, however, indicates possible correlations between tropospheric gradients and other estimated parameters, such as ambiguities, height and zenith total delays, and suggests a careful handling particularly when applying a sub-daily temporal resolution.

5.5 Spatial and temporal ZTD analysis

We performed spatial and temporal analyses of all processed variants in order to assess the impact of different settings on tropospheric products. Zenith tropospheric delays from all variants were compared in such a way to enable assessing impact of any single processing change: 1) GO1-GO0 for mapping function and more precise a priori ZHD model, 2) GO2-GO1 and GO3-GO1 for different elevation cut-off angle, 3) GO4-GO1 for non-tidal atmospheric corrections, 4) GO5-GO4 for higher-order ionospheric corrections and, 5) GO6-GO4 for temporal resolution tropospheric horizontal gradients. Station-specific behavior ~~is out of this paper and~~ will be studied in future.

Geographical maps of spatially distributed biases and standard deviations in ZTDs from all compared variants for the whole network are ~~showed~~ in Figure 10 and Figure 11. Additionally median, minimum and maximum values of station-wise total statistics are provided in Table 5. ~~The comparisons demonstrated that the impact of the higher-order effect is fully negligible. Although overall mean biases in Table 5 are small, the GO1-GO0 comparison indicates a small negative bias over a majority of the stations, see Figure 10. Biases from the comparison of variants with different elevation cut-off angles strongly indicates a station-specific behavior with a positive bias for stations around Poland, which has not been explained yet. According to the table and Figure 11, the highest impact on standard deviations is found in the GO1 vs. GO0 solutions comparison. The effect is latitude dependent and it follows the increasing magnitude of ZTDs towards the equator. Detailed study illustrated in~~ Figure 12, Figure 13 and Figure 14 ~~then~~ illustrates ZTD statistics with respect to the station latitude, ellipsoidal height and time, respectively.

Using VMF1 mapping function together with precise a priori ZHD from VMF1 instead of the GMF and GPT models, respectively, see GO1 vs. GO0, we observe biases ranging from -1.52 to 0.70 mm and the median value -0.36 mm and, according to Table 5, with a moderate latitudinal dependence, see Figure 12. ~~A similar, but slightly larger negative bias of -0.94±0.28 mm, was reported Kacmarik et al. (2017) studying 400 stations in the central Europe~~. Standard deviations range from 0.69 mm to 3.82 mm in Table 5 with a ~~profound~~ increase along with the latitude, Figure 12, indicating the GPT performs worse at higher latitudes. This ~~fully corresponds to the results from the paper by~~ Steigenberger et al. (2009) demonstrating a partial compensation of the atmospheric loading effect by using the GPT model. In case the atmospheric loading effect is not corrected for, the errors are mostly assimilated to the zenith total delay parameters if station coordinates are fixed on a weekly basis. Additionally, Figure 14 shows the standard deviation grows with time ~~which can be attributed to the use of blind (GMF) and actual-weather (VMF1) mapping functions. The mapping function affects an optimal use of~~ low-elevation observations, which were growing in EUREF permanent network with time as demonstrated for WTZR station in Figure 15.

Biases obtained from the comparison of different elevation cut-off angles, i.e. variants 3°/7° (GO2-GO1) and 3°/10° (GO3-GO1), range from -0.81 mm to 1.66 mm and -2.22 mm to 2.66 mm, respectively, and standard deviations from 0.15 mm to 1.29 mm and 0.31 to 2.04 mm, see Table 5. Generally, the impact of different elevation cut-off angle doesn't reveal any biases neither with respect to the latitude (Figure 12) nor the station height (Figure 13). As expected, the impact is larger for the GO3-GO1 differences and affected particularly some stations. Yearly biases exceeding ±2.5 mm were identified for BELL, DENT, MLVL, MOPS, POLV RAMO and SBG2 stations. Temporal dependences in the GO2-GO1 and GO3-GO1 comparisons, Figure 14, show that the scatter of station-specific biases steadily grows in time which is assumed to be related to the higher availability of low-elevation observations. On the other hand, a small impact is observed for the standard deviation compared to the other studied effects. This indicates the elevation cut-off angle affects mainly ZTD biases, which has been also reported by Ning and Elgered (2012).

Table 5 shows that biases due to the non-tidal atmospheric loading (GO4-GO1) range from -2.29 mm to 5.55 mm, which is one of the largest impact compared to other comparison variants, and standard deviations range from 0.68 mm to 4.72 mm that represents the second largest impact compared to all other variants. Standard deviation larger than 3 mm was observed at some stations, such as JOZE, MAD2, MADR, MDVO, MOPI, NYAL, SBG2, VENE and WETT. It should be emphasized this comparison reflects differences due to the modelling of atmospheric loading corrections in GO4 and, a partial compensation of the loading effect by zenith tropospheric delay estimates in the GO1 solution variant. The differences are strongly station-dependent, but did not reveal any dependence on latitude, see Figure 12. It shows, however, some degradation in standard deviation during the first years of the reprocessing, see Figure 14. Since a similar degradation has not been observed for other comparison variants, it can be related to the quality of pressure data used to compute atmospheric loading.

The impact of higher-order ionospheric effect (GO5-GO4) is negligible at all stations demonstrating total statistics for all stations within ±0.3 mm when applying the y-range about 10 times smaller than in other panels of Figure 12, Figure 13 and Figure 14. A strong latitudinal dependence is, however, clearly visible in Figure 12 as well as a temporal variability showing ~~yearly statistics~~ up to ±0.4 mm, Figure 14. Both dependences are due to the changing magnitude of ionospheric corrections, generally

increasing towards the equator ~~and a daily noon, and~~ along with cycles of the solar magnetic activity, reaching peaks around years 2001 and 2014.

The impact of stacking tropospheric gradients from 6-hour to daily estimates (GO6-GO4) is almost negligible in term of biases which stay below ±1 mm, Table 5 and Figure 10. However, standard deviations range from 0.76 mm to 2.46 mm and grow towards the equator, Figure 12. That can be certainly attributed to the more difficult modelling of a local asymmetry in the troposphere, which is generally increasing together with the increasing of the water vapor content. There is no significant temporal variation observed ~~in Figure 14,~~ but a small decrease in standard deviation. It can be attributed to a higher stability of the gradient estimates with time, see Figure 9, when supported with increased number of available low-elevation observations.

6 Impact of variants on long-term ZTD trend estimates

We assessed the impact of solution variant on long-term ZTD trend estimates by analysing 172 EUREF stations providing the time-series of data longer than 10 years. For each station, the trend analysis was performed without any data homogenization or outlier rejection as our focus was only on assessing the impact of solution variants on the trend estimates. The ZTD trends were estimated using the least squares regression method applied on model (Weatherhead et al., 1998)

$$Y_t = \mu + \beta X_t + S_t + \varepsilon_t \quad (2)$$

where μ is the constant term of the model, βX_t is the linear trend function with β representing the trend magnitude, S_t represents the term modelled by the sine wave function of time X_t including annual, 2nd harmonics and daily variations, and finally ε_t is the noise in the data.

Site-by-site estimated ZTD trends from all the variants are provided in supplementary materials completed by time-span information, number of records and estimated mean formal errors calculated over all variants. In total, trends range from -0.99 to 0.96 mm/year. Although the individual station trend provided in supplements could be compared to other studies, e.g. Baldysz et al. (2016), Klos et al. (2016) or Nilsson and Elgered (2008), however, it should be strongly emphasized here that our trends are estimated without any preceding time-series homogenization and the formal errors of the trend estimates are underestimated by a factor 2-4 (Nilsson and Elgered, 2008).

Table 6 summarizes the statistics of estimated trend differences at all 172 stations, always between particular variants as defined in Section 5.5. Interestingly, the most significant impact is observed due to the non-tidal atmospheric loading effects reaching differences ~~up to~~ ±0.55 mm/year in ZTD trends for some extreme cases from the ensemble of 172 stations, and an overall scatter of 0.50 mm/year from the ensemble of stations. Changes in elevation cut-off angle, particularly from 3° to 10°, reveal also a significant impact characterized by differences ~~up to~~ ±0.34 mm/year and the scatter of 0.32 mm/year. The impact of mapping function on trend estimates remains small, with a maximum difference of 0.12 mm/year and the scatter below 0.08 mm/year, while other strategy changes, due to time resolution of tropospheric gradients and higher-order ionospheric effects, remains negligible, always below ±0.04 mm/year for all 172 stations, with the scatter of the same magnitude. All mean biases over differences stay also below 0.05 mm/year.

Finally, we selected 12 stations ~~optimally~~ available over the entire 2nd re-processing period ~~and all~~ estimated trends are displayed in Figure 16. ~~Trends for 12 stations~~ range from -0.05 to 0.38 mm/year ~~with formal errors of 0.02-0.04 mm/year. It should be noted the formal errors are underestimated by a factor of 2-4 because the noise is assumed white (Nilsson and Elgered (2008). For the 12 selected stations,~~ the most significant impact is observed in the change of elevation cut-off angle when reaching differences up to 0.1 mm/year in estimated ZTD trends. ~~A similar, but more extensive study, was performed by Ning and Elgered (2012) for Integrated Water Vapor content (IWV), roughly equal to 1/6 (ZTD-ZHD) kg.m^{-2}, using larger differences in the elevation cut-off angle and obtaining highly sensitive results in term of estimated IWV trends.~~ Impacts of other strategies are generally below 0.05 mm/year – variants GO4, GO5, and GO6 are very similar, but not consistent again with GO1, meaning the non-tidal atmospheric loading has a significant impact on trend estimates for selected stations with the longest data time-series.

7 Conclusions

In this paper, we present results of the new GOP reanalysis of all stations within the EUREF Permanent network during the period of 1996-2014. This reanalysis was completed during the 2nd EUREF reprocessing to support the realization of a new European terrestrial reference system. In the 2nd reprocessing, we focused on analysing a new product – GNSS tropospheric parameter time-series for applications to climate research. To achieve this goal, we improved our strategy for combining tropospheric parameters at midnights and at transitions in GPS weeks. We also performed seven solution variants to study optimal troposphere modelling; we assessed each of these variants in terms of their coordinate repeatability by using internal evaluations of the applied models and strategies. We also compared tropospheric ZTD and tropospheric horizontal gradients with independent evaluations obtained by numerical weather reanalysis via the ERA-Interim.

Results of the GOP Repro2 yielded improvements of approximately 50% and 25% for their horizontal and vertical component repeatability, respectively, when compared to those of the GOP Repro1 solution. Vertical repeatability was reduced from 4.14 mm to 3.73 mm when using the VMF1 mapping function, a priori ZHD, and non-tidal atmospheric loading corrections from actual weather data. Increasing the elevation cut-off angle from 3° to 7°/10° increased RMS errors of residuals from these coordinates' repeatability. All of these factors were also confirmed by the independent assessment of tropospheric parameters using NWM reanalysis data.

We particularly recommend using low-elevation observations along with the VMF1 mapping function, as well as using precise a priori ZHD values together with the consistent model of non-tidal atmospheric loading. While estimating tropospheric horizontal linear gradients improves coordinates' repeatability, 6-hour sampling without any absolute or relative constraints revealed a loss of stability due to their correlations with other parameters. On the other hand, 24-h piecewise linear gradients did not indicate a worse repeatability of coordinates estimates. For saving the time needed for the processing of 4 times less gradient parameters, we could recommend as sufficient using unconstrained 24-h piecewise model for the first-order tropospheric asymmetry.

The impact of processing variants on long-term ZTD trend estimates was assessed at 172 EUREF stations with time-series longer than 10 years. The most significant impact was observed due to the non-tidal atmospheric loading effect reaching differences ~~up to~~ ±0.55 mm/year in ZTD trends for some

extreme cases from the ensemble of 172 stations. Changes in elevation cut-off angle, particularly from 3° to 10°, revealed also a significant impact reaching differences ~~up to~~ ±0.35 mm/year. The change of mapping function was observed rather small, with a maximum difference of 0.12 mm/year, while other strategy changes, due to time resolution of tropospheric gradients and higher-order ionospheric effects, remained negligible, always below ±0.04 mm/year for all 172 stations.

Assessing the tropospheric horizontal gradients with respect to the ERA-Interim reanalysis data revealed some long-term systematic behaviour linked to degradation in antenna tracking quality. We presented an extreme case at the Mallorca station (MALL), in which gradients systematically increased up to 5 mm from 2003-2008 while pointing in the direction of prevailing observations at low elevation angles. However, these biases disappeared when the malfunctioning antenna was replaced. More cases similar to this, although less extreme, have indicated that estimated tropospheric gradients are extremely sensitive to the quality of GNSS antenna tracking, thus suggesting that these gradients can be used to identify problems with GNSS data tracking in historical archives.

One of the main difficulties faced during the 2nd reprocessing was that of the quality of the historical data, which contains a large variety of problems. We removed data that caused significant problems in network processing when these could not be pre-eliminated from normal equations during the combination process without still affecting daily solutions. To provide high-accuracy, high-resolution GNSS tropospheric products, the elimination of such problematic data or stations is even more critical considering the targeting static coordinates on a daily or weekly basis for the maintenance of the reference frame or the derivation of a velocity field. Before undertaking the 3rd EUREF reprocessing, which is expected to begin after significant improvements have been made to state-of-the-art models, products and software, we need to improve data quality control and clean the EUREF historical archive in order to optimize any future reprocessing efforts and to increase the quality of tropospheric products. These efforts should also include the collection and documentation of all available information from each step of the 2nd EUREF reprocessing, including individual contributions, EUREF combinations, time-series analyses and coordinates, and independent evaluations of tropospheric parameters.

Acknowledgments

The reprocessing effort and its evaluations were supported by the Ministry of Education, Youth and Science, the Czech Republic (projects LD14102 and LO1506). We thanks two anonymous reviewers and Dr. Olivier Bock for comments and suggestions which helped us to improve the manuscript.

References

- Altamimi, Z., Angermann, D., Argus, D., et al.: The terrestrial reference frame and the dynamic Earth, EOS, Transacttions, American Geophysical Union, 82, 273–279, 2001.
- Baldysz, Z., Nykiel, G., Araszkiewicz, A., Figurski, M., and Szafranek, K., Comparison of GPS tropospheric delays derived from two consecutive EPN reprocessing campaigns from the point of view of climate monitoring, Atmos. Meas. Tech., 9, 4861-4877, 2016.
- Bevis, M., Businger, S., Chiswell, S., Herring, T. A., Anthes, R. A., Rocken C, and Ware R. H.: GPS Meteorology: Mapping Zenith Wet Delays onto Precipitable Water, J. Appl. Meteorol., 33, 379–386, 1994.

- Bock, O., Willis, P., Wang, J., and Mears, C.: A high-quality, homogenized, global, long-term (1993–2008) DORIS precipitable water data set for climate monitoring and model verification, J. Geophys. Res. Atmosphere, 119, 7209–7230, 2014.
- Bock, O., and Nuret, M.: Verification of NWP model analyses and radiosonde humidity data with GPS precipitable water vapor estimates during AMMA, Weather and Forecasting, 24(4), 1085-1101, 2009.
- Bock, O., Bosser, P., Pacione, R., Nuret, M., Fourrié, N., and Parracho, A.: A high-quality reprocessed ground-based GPS dataset for atmospheric process studies, radiosonde and model evaluation, and reanalysis of HyMeX Special Observing Period. Q.J.R. Meteorol. Soc., 142, 56–71, 2016.
- Böhm, J., Niell, A. E., Tregoning, P., and Schuh, H.: 2006, Global Mapping Functions (GMF): A new empirical mapping function based on numerical weather model data, Geophys. Res. Lett., 33, L07304, 2006a.
- Böhm, J., Werl, B., and Schuh, H.: Troposphere mapping functions for GPS and very long baseline interferometry from European Centre for Medium-Range Weather Forecasts operational analysis data. J. Geophys. Res., 111, B02406, 2006b.
- Bruyninx, C., Habrich, H., Söhne, W., Kenyeres, A., Stangl, G., and Völksen, C.: Enhancement of the EUREF Permanent Network Services and Products, Geodesy for Planet Earth, IAG Symposia Series, 136, 27–35, 2012.
- Dach, R., Böhm, J., Lutz, S., Steigenberger, P., and Beutler, G.: Evaluation of the impact of atmospheric pressure loading modeling on GNSS data analysis, J. Geod., 85(2), 75–91, 2011.
- Dach, R., Schaer, S., Lutz, S., Baumann, C., Bock, H., Orliac, E., Prange, L., Thaller, D., Mervart, L., Jäggi, A., Beutler, G., Brockmann, E., Ineichen, D., Wiget, A., Weber, G., Habrich, H., Söhne, W., Ihde, J., Steigenberger, P., and Hugentobler, U.: CODE IGS Analysis Center Technical Report 2013, Dach, R., and Jean, Y. (eds.), IGS 2013 Tech. Rep., 21–34, 2014.
- Dach, R., Lutz, S., Walser, P., and Fridez, P. (Eds.): Bernese GNSS Software Version 5.2. User manual, Astronomical Institute, University of Bern, Bern Open Publishing, 2015.
- Dee, D.P., Uppala, S.M., Simmons, A.J. et al.: The ERA-Interim reanalysis: Configuration and performance of the data assimilation system, Q. J. Roy. Meteorol. Soc., 137, 553–597, 2011.
- Douša, J., and Václavovic, P.: Results of GPS Reprocessing campaign (1996-2011) provided by Geodetic observatory Pecný, Geoinformatics, FCE CTU, 9, 77–89, 2012.
- Douša, J., Dick, G., Kačmařík, M., Brožková, R., Zus, F., Brenot, H., Stoycheva, A., Möller, G., and Kaplon, J.: Benchmark campaign and case study episode in central Europe for development and assessment of advanced GNSS tropospheric models and products, Atmos. Meas. Tech., 9, 2989–3008, 2016.
- Douša, J., Böhm, O., Byram, S., Hackman, C., Deng Z., Zus, F., Dach, R., and Steigenberger, P.: Evaluation of GNSS reprocessing tropospheric products using GOP-TropDB, IGS Workshop 2016, Sydney, February 8–12, 2017, available at: http://www.igs.org/assets/pdf/W2016%20-%20PS0303%20-%20Dousa.pdf
- Fritsche, M., Dietrich, R., Knofel, C., Rülke, A., Vey, S., Rothacher, M., and Steigenberger, P.: Impact of higher-order ionospheric terms on GPS estimates. Geophys. Res. Lett., 32, L23311, 2005.

- Győri, G., and Douša, J.: GOP-TropDB developments for tropospheric product evaluation and monitoring – design, functionality and initial results, IAG Symposia Series, Springer, 143, 595–602, 2016.
- Ihde, J., Habrich, H., Sacher, M., Sohne, W., Altamimi, Z., Brockmann, E., Bruyninx, C., Caporali, A., Dousa, J., Fernandes, R., Hornik, H., Kenyeres, A., Lidberg, M., Makinen, J., Poutanen, M., Stangl, G., Torres, J.A., and Volksen, C.: EUREF's Contribution to National, European and Global Geodetic Infrastructures, In: Earth on the Edge: Science for a Sustainable Planet, Rizos, C. and Willis P. (eds), IAG Symposia Series, Springer, 139, 189–196, 2014.
- IERS Conventions: Gérard, P., and Luzum, B. (Eds.), IERS Technical Note No. 36, Frankfurt am Main: Verlag des Bundesamts für Kartographie und Geodäsie, 179 pp., 2010.
- Kačmařík, M., Douša, J., Dick, G., Zus, F., Brenot, H., Möller, G., Pottiaux, E., Kapłon, J., Hordyniec, P., Václavovic, P., and Morel, L.: Inter-technique validation of tropospheric slant total delays, Accepted for Atmos. Meas. Tech. 2017.
- Klos, A., Hunegnaw, A., Teferle, F. N., Abraha, K. E., Ahmed, F., and Bogusz, J., Noise characteristics in Zenith Total Delay from homogeneously reprocessed GPS time series, Atmos. Meas. Tech. Discuss., 2016.
- Li, X., Zus, F., Lu, C., Ning, T., Dick, G., Ge, M., Wickert, J., and Schuh, H.: Retrieving high-resolution tropospheric gradients from multiconstellation GNSS observations, Geophys. Res. Lett., 42(10), 4173–4181, 2015.
- Meindl, M., Schaer, S., Hugentobler, U., and Beutler, G.: Tropospheric Gradient Estimation at CODE: Results from Global Solutions. Journal of the Meteorological Society of Japan, 82, 331–338, 2004.
- Morel, L., Pottiaux, E., Durand, F., Fund, F., Follin, J.M., Durand, S., Bonifac, K., Oliveira, P.S., van Baelen, J., Montibert, C., Cavallo, T., Escaffit, R., and Fragnol, L.: Global validity and behaviour of tropospheric gradients estimated by GPS, presentation at the 2nd GNSS4SWEC Workshop held in Thessaloniki, Greece, May 11–14, 2015.
- MacMillan, D. S.: Atmospheric gradients from very long baseline interferometry observations, Geophys. Res. Lett., 22, 1041–1044, 1995.
- Meindl, M., Schaer, S., Hugentobler, U., and Beutler, G.: Tropospheric Gradient Estimation at CODE: Results from Global Solutions. J. Meteorol. Soc. Japan, 82, 331–338, 2004.
- Nilsson, T., and Elgered, G., Long-term trends in the atmospheric water vapor content estimated from ground-based GPS data, J. Geophys. Res., 113, D19101, 2008.
- Ning, T.: GPS Meteorology: With Focus on Climate Applications, PhD Thesis, Dept. Earth and Space Sciences. Chalmers University of Technology, 2012.
- Ning, T., and Elgered, E.: Trends in the atmospheric water vapor content from ground-based GPS: The impact of the elevation cutoff angle, IEEE J. Sel. Top. Appl. Earth Obs. Remote Sens., 5, 744–751, 2012.
- Pacione, R., Araszkiewicz, A., Brockmann, E., and Dousa, J.: EPN-Repro2: A reference GNSS tropospheric data set over Europe, Atmos. Meas. Tech., 10, 1689–1705, doi:10.5194/amt-10-1689-2017, 2017.
- Steigenberger, P., Böhm, J., and Tesmer, V.: Comparison of GMF/GPT with VMF1/ECMWF and implications for atmospheric loading, J. Geod., 83, 943, 2009.

- Václavovic, P., and Douša, J.: G-Nut/Anubis – open-source tool for multi-GNSS data monitoring, In: IAG 150 Years, Rizos, Ch. and Willis, P. (eds), IAG Symposia Series, Springer, 143, 775–782, 2016.
- Völksen, C.: An update on the EPN Reprocessing Project: Current Achievements and Status, Presented at the EUREF 2011 Symposium, Chisinau, Republic of Moldova, May 25–28. http://www.epncb.oma.be/_documentation/papers/eurefsymposium2011/an_update_on_epn_reprocessing_project_current_achievement_and_status, 2011
- Weatherhead, E. C., Reinsel, G. C., Tiao, G. C. et al.: Factors affecting the detection of trends: Statistical considerations and applications to environmental data, J. Geophys. Res., 103(D14), 17149–17161, 1998.
- Yuan, L.L., Anthes, R.A., Ware, R.H., Rocken, C., Bonner, W.D., Bevis, M.G., and Businger, S.: Sensing Climate Change Using the Global Positioning System, J. Geophys. Res., 98, 14925–14937, 1993.
- Zus, F., Dick, G., Heise, S., Dousa, J., and Wickert, J.: The rapid and precise computation of GPS slant total delays and mapping factors utilizing a numerical weather model, Radio Sci., 49, 207–216, 2014.
- Zus, F., Dick, G., Dousa, J., and Wickert, J.: Systematic errors of mapping functions which are based on the VMF1 concept, GPS Solut., 19(2), 277–286, 2015.

718 **Table 1: Characteristics of GOP reprocessing models**

Processing options	Description
Products	CODE precise orbit and earth rotation parameters from the 2nd reprocessing.
Observations	Dual-frequency code and phase GPS observations from L1 and L2 carriers. Elevation cut-off angle 3°, elevation-dependent weighting $1/\cos^2$ (zenith), double-difference observations and with 3-minute sampling rate.
Reference frame	IGb08 realization, core stations set as fiducial after a consistency checking. Coordinates estimated using a minimum constraint.
Antenna model	GOP: IGS08_1832 model (receiver and satellite phase centre offsets and variations).
Troposphere	A priori zenith hydrostatic delay/mapping function: GPT/GMFh (GO0) and VMF1/VMF1h (GO1-GO6). Estimated ZWD corrections every hour using VMF1 wet mapping function; 5 m and 1 m for absolute and relative constraints, respectively. Estimated horizontal NS and EW tropospheric gradients every 6 hours (GO0-GO5) or 24 hours (GO6) without a priori tropospheric gradients and constraints.
Ionosphere	Eliminated using ionosphere-free linear combination (GO0-GO6). Applying higher-order effects estimated using CODE global ionosphere product (GO5).
Loading effects	Atmospheric tidal loading and hydrology loading not applied. Ocean tidal loading FES2004 used. Non-tidal atmospheric loading introduced in advanced variants from the model from TU-Vienna (GO4-GO6).

719

720 **Table 2: GOP solution variants for the assessment of selected models and settings**

Solution ID	Specific settings and differences	Remarks and rationales
GO0	GMF and 3° cut-off	Legacy solution for Repro1
GO1	VMF1 and 3° cut-off	New candidate for Repro2
GO2	=GO1; 7° cut-off	Impact of elevation cut-off angle
GO3	=GO1; 10° cut-off	Impact of elevation cut-off angle
GO4	=GO1; atmospheric loading	Non-tidal atmospheric loading applied
GO5	=GO4; higher-order ionosphere	Higher-order ionosphere effect not applied
GO6	=GO4; 24-hour gradients	Stacking tropospheric gradients to 24-hour sampling

721

722 **Table 3: Comparison of GOP solution variants for north, east and up coordinate repeatability.**

Solution	North RMS [mm]	East RMS [mm]	Up RMS [mm]
GOP-Repro1/IGS05	3.01	2.40	5.08
GOP-Repro1/IGS08	2.64	2.21	4.94
GO0	1.20	1.30	4.14
GO1	1.23	1.33	3.97
GO2	1.24	1.33	4.01
GO3	1.26	1.34	4.07
GO4	1.14	1.24	3.73
GO5	1.14	1.24	3.73
GO6	1.14	1.24	3.73

723

724 **Table 4: Statistics (bias and standard deviations) of ZTD and tropospheric gradients from the seven reprocessing variants**
725 **compared to those obtained from the ERA-Interim NWM reanalysis. In addition to the statistics, 1-sigma range over**
726 **ensemble of stations is provided.**

Solution	ZTD bias [mm]	ZTD sdev [mm]	EGRD bias [mm]	EGRD sdev [mm]	NGRD bias [mm]	NGRD sdev [mm]
GO0	-1.5 ± 2.1	8.8 ± 2.0	-0.04 ± 0.08	0.39 ± 0.10	+0.01 ± 0.09	0.43 ± 0.12
GO1	-2.0 ± 2.1	8.3 ± 2.2	-0.04 ± 0.08	0.39 ± 0.10	+0.01 ± 0.09	0.42 ± 0.13
GO2	-1.9 ± 2.2	8.4 ± 2.2	-0.05 ± 0.10	0.41 ± 0.10	+0.00 ± 0.12	0.45 ± 0.12
GO3	-1.8 ± 2.3	8.5 ± 2.1	-0.08 ± 0.13	0.43 ± 0.11	-0.01 ± 0.14	0.49 ± 0.12
GO4	-1.8 ± 2.4	8.1 ± 2.1	-0.04 ± 0.09	0.38 ± 0.10	+0.00 ± 0.09	0.40 ± 0.12
GO5	-1.8 ± 2.4	8.1 ± 2.1	-0.05 ± 0.09	0.38 ± 0.10	+0.01 ± 0.08	0.40 ± 0.12
GO6	-1.8 ± 2.4	8.2 ± 2.1	-0.04 ± 0.08	0.29 ± 0.06	+0.01 ± 0.09	0.28 ± 0.06

727

728 **Table 5: Median, minimum (min) and maximum (max) values of total ZTD biases and standard deviation (sdev) over all**
729 **stations. Units are millimetres.**

Compared variants	ZTD bias median	ZTD bias min	ZTD bias max	ZTD sdev median	ZTD sdev min	ZTD sdev max
GO1-GO0	-0.36	-1.52	+0.70	2.01	0.69	3.82
GO2-GO1	+0.03	-0.81	+1.66	0.66	0.15	1.29
GO3-GO1	+0.03	-2.22	+2.66	1.10	0.31	2.04
GO4-GO1	+0.05	-3.29	+5.55	1.37	0.68	4.72
GO5-GO4	-0.02	-0.31	+0.07	0.07	0.04	0.30
GO6-GO4	-0.02	-0.23	+0.16	1.24	0.76	2.46

730

731 **Table 6: Mean statistics of ZTD trends differences estimated between variants for 172 stations. Units are millimetres/year.**

Statistics	GO1-GO0	GO2-GO1	GO3-GO1	GO4-GO1	GO5-GO4	GO6-GO4
Min	-0.118	-0.141	-0.308	-0.547	-0.017	-0.038
Max	0.045	0.179	0.331	0.452	0.031	0.036
mean	0.036	0.018	0.012	-0.048	0.007	0.001
Sdev	0.081	0.160	0.319	0.499	0.024	0.037

732

733

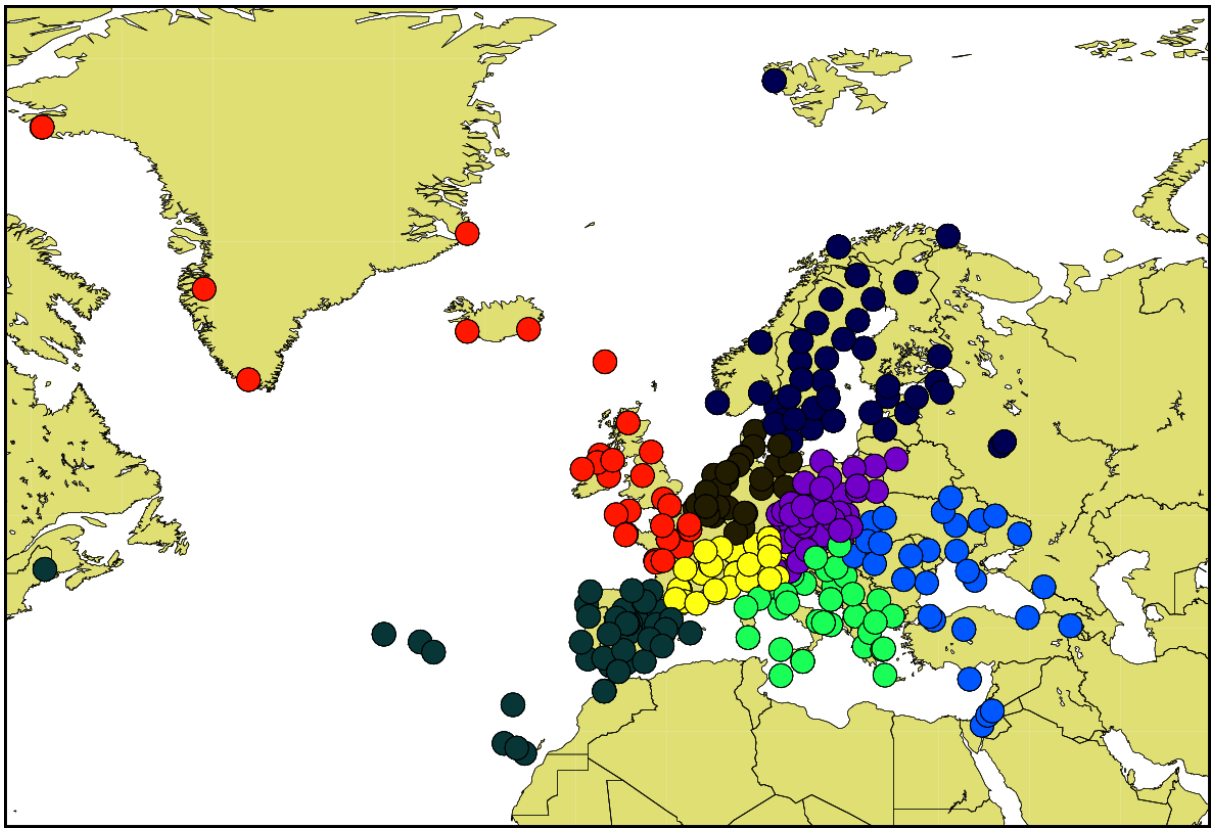

Figure 1: EUREF Permanent Network's clusters (designated by different colours) in the 2nd GOP reprocessing.

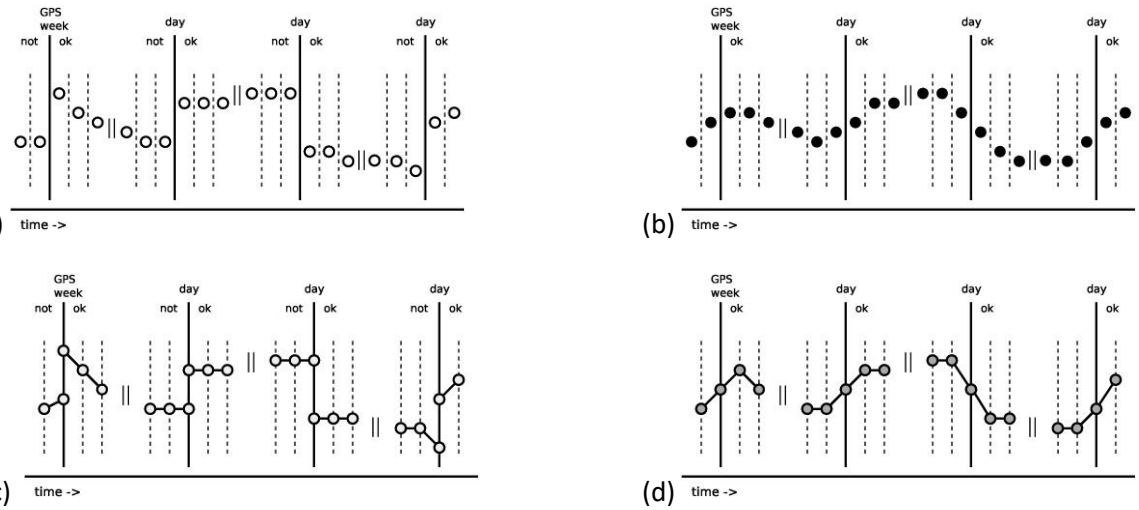

Figure 2: Charts of 4 variations on representations of tropospheric parameters. Right (b), (d) and left (a), (c) panels display estimates made with and without midnight combinations, respectively. Top (a), (b) and bottom (c), (d) panels display the piecewise constant and the linear model, respectively.

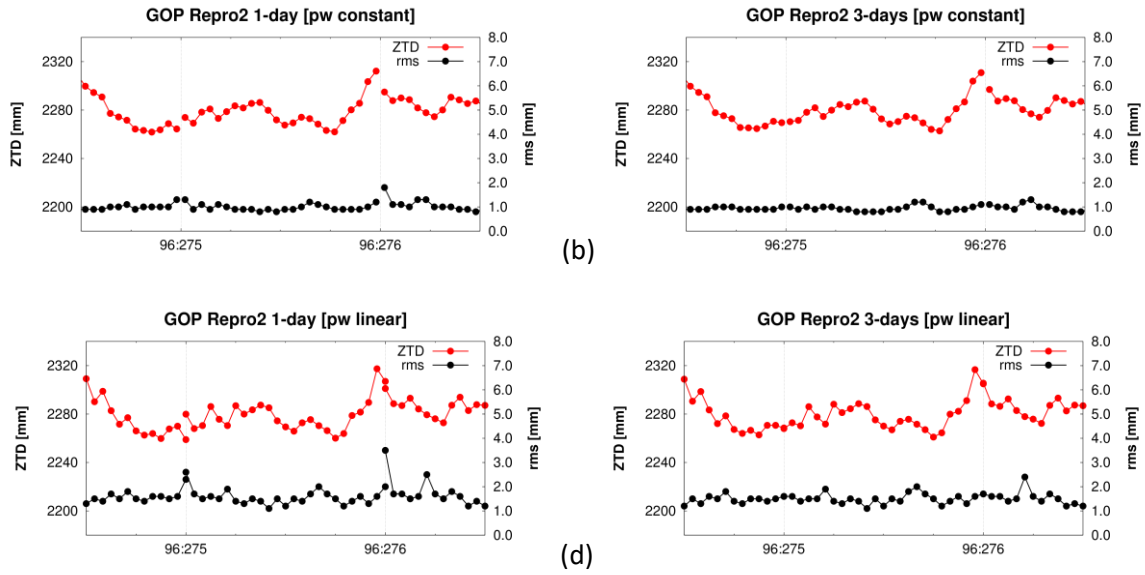

743 (a) (b)

744 (c) (d)

745 Figure 3: Four variations in representation of tropospheric parameters. Right (b), (d) and left (a), (c)
746 panels display estimates with and without midnight combinations, respectively. Top (a), (b) and
747 bottom (c), (d) panels display the piecewise constant and the piecewise linear model, respectively.

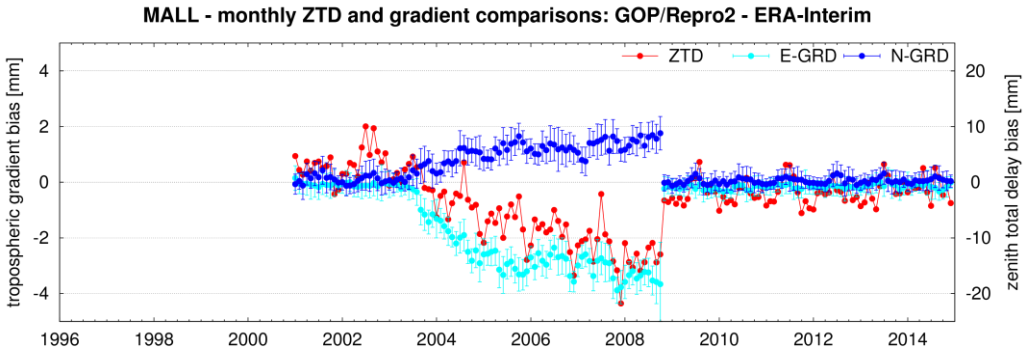

748
749 **Figure 4: MALL station - monthly mean differences in tropospheric horizontal gradients with respect to the ERA-Interim.**

750

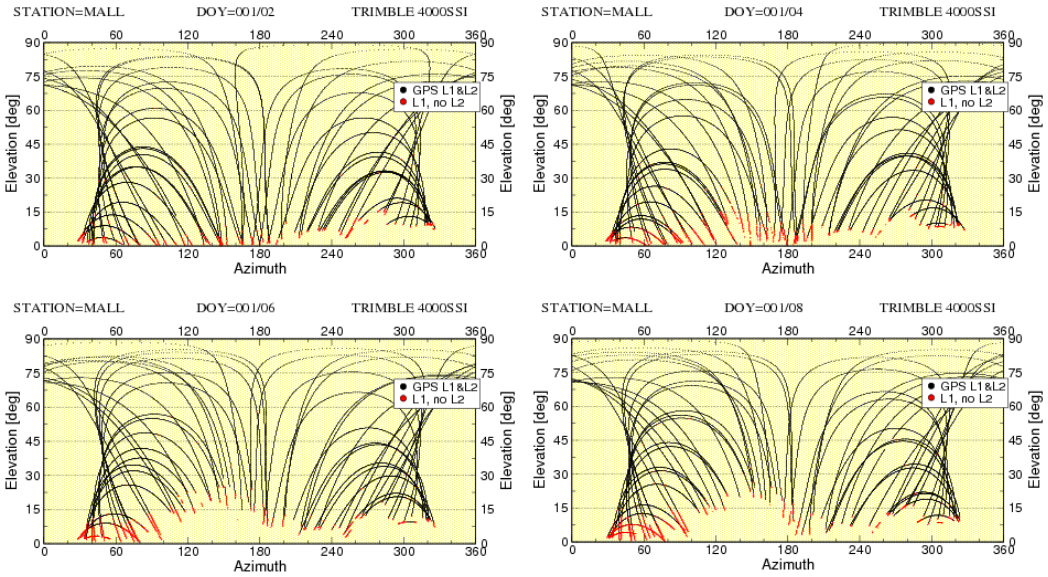

751

752

753 **Figure 5: Low-elevation tracking problems at the MALL station during the period of 2003-2008. From left-top to right-**
754 **bottom: January 2002, 2004, 2006 and 2008 (courtesy of the EPN Central Bureau, ROB).**

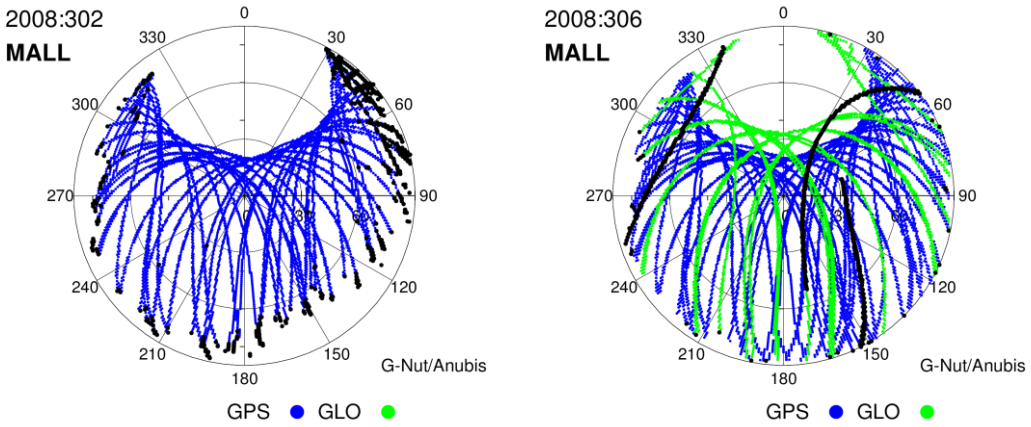

755

756 **Figure 6: Sky plots before (left) and after (right) replacing the malfunctioning antenna at the MALL site (Oct 30, 2008).**
757 **Black dots indicates single-frequency observations available only.**

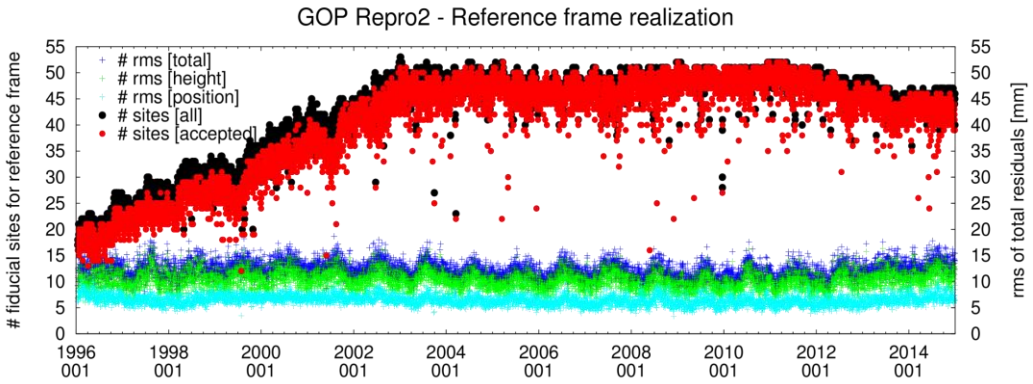

Figure 7: Statistics of the daily reference system realization: a) RMS of residuals at fiducial stations (representing the total, height and position); b) number of stations (all and accepted after an iterative control)

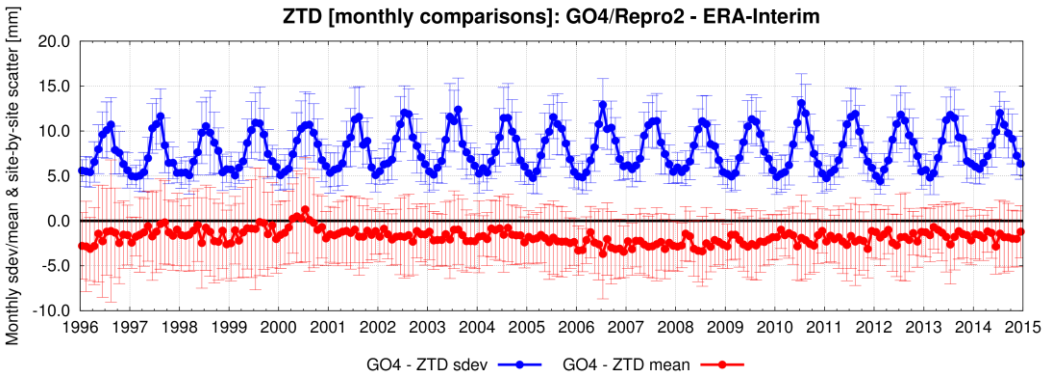

762

763 **Figure 8: Monthly means of bias and standard deviation of official GOP ZTD product compared to those of the ERA-Interim.**
764 **Error bars indicate standard errors of mean values over all compared stations.**

765

766

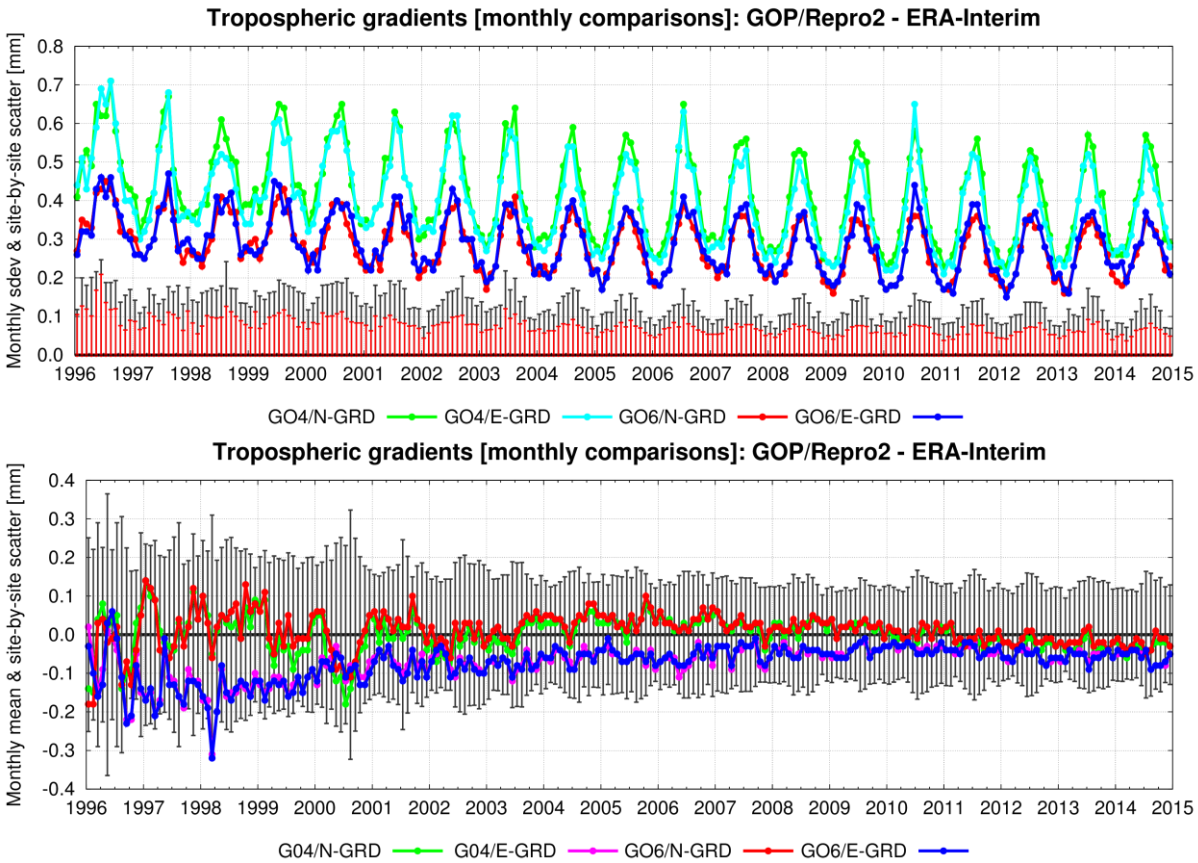

Figure 9: Monthly means of bias and standard deviation of tropospheric horizontal north (N-GRD) and east (E-GRD) gradients compared to those obtained by ERA-Interim. Note: Similar products are almost superposed. Error bars indicate standard errors of mean values over all compared stations plotted from the zero y-axis to emphasise seasonal variations and trends. Error bars are displayed for north gradients only, however, being representative for the east gradients too.

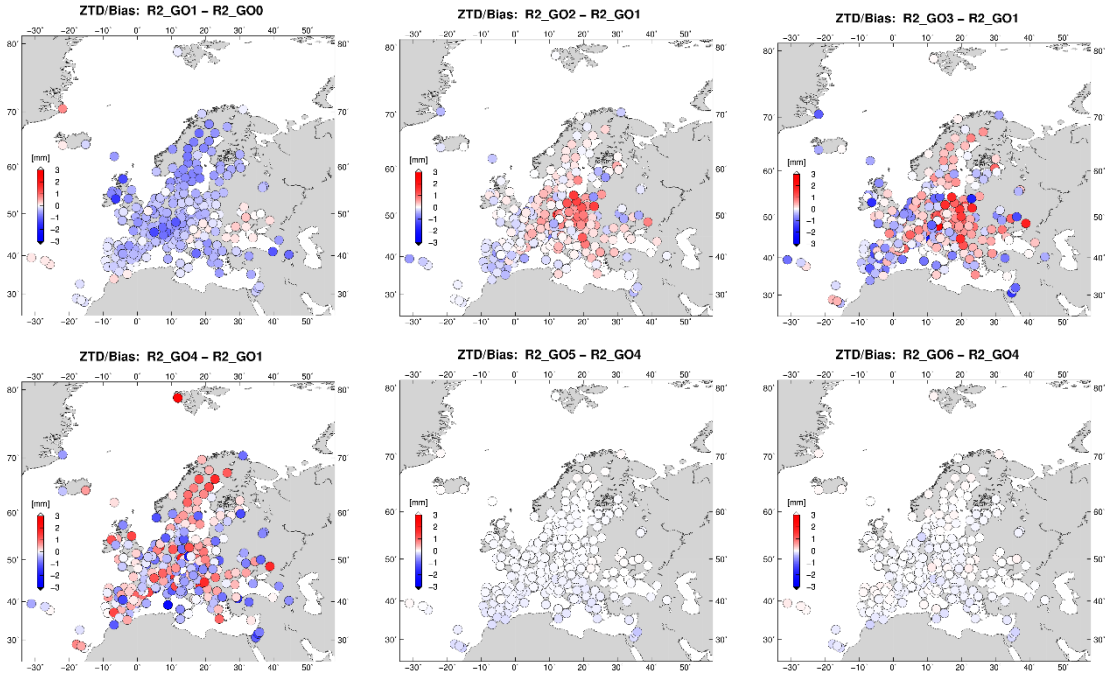

773

774
775 **Figure 10: Geographic visualization of biases from inter-comparisons of GOP 2nd reprocessing variants.**

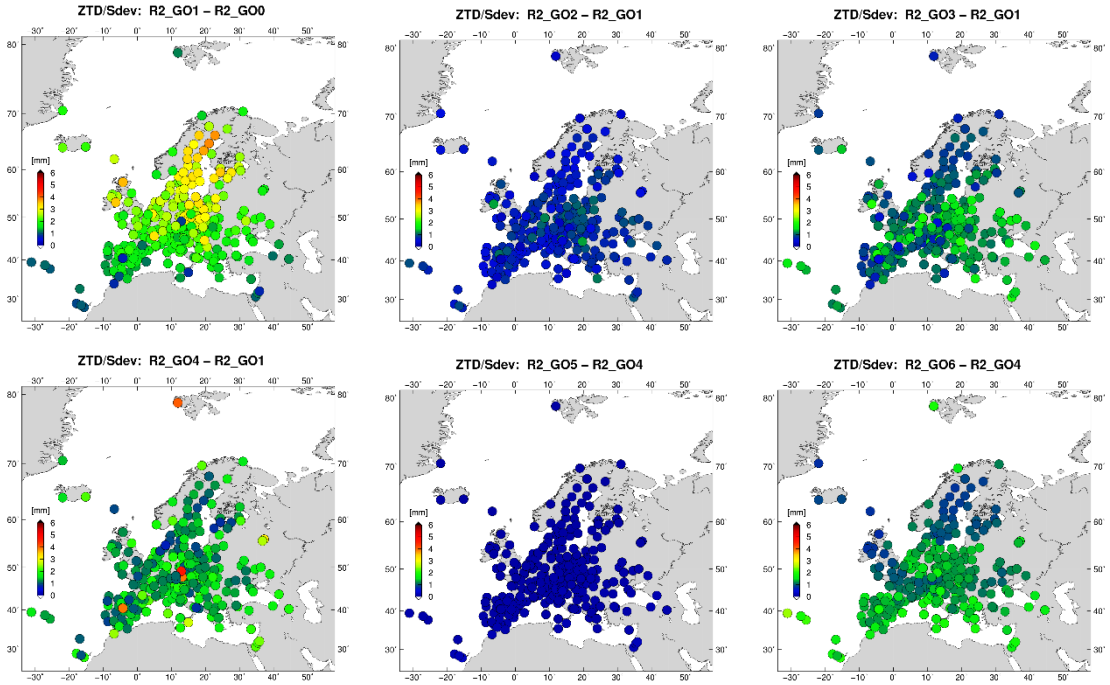

776

777

778 **Figure 11: Geographic visualization of standard deviations from inter-comparisons of GOP 2nd reprocessing variants.**

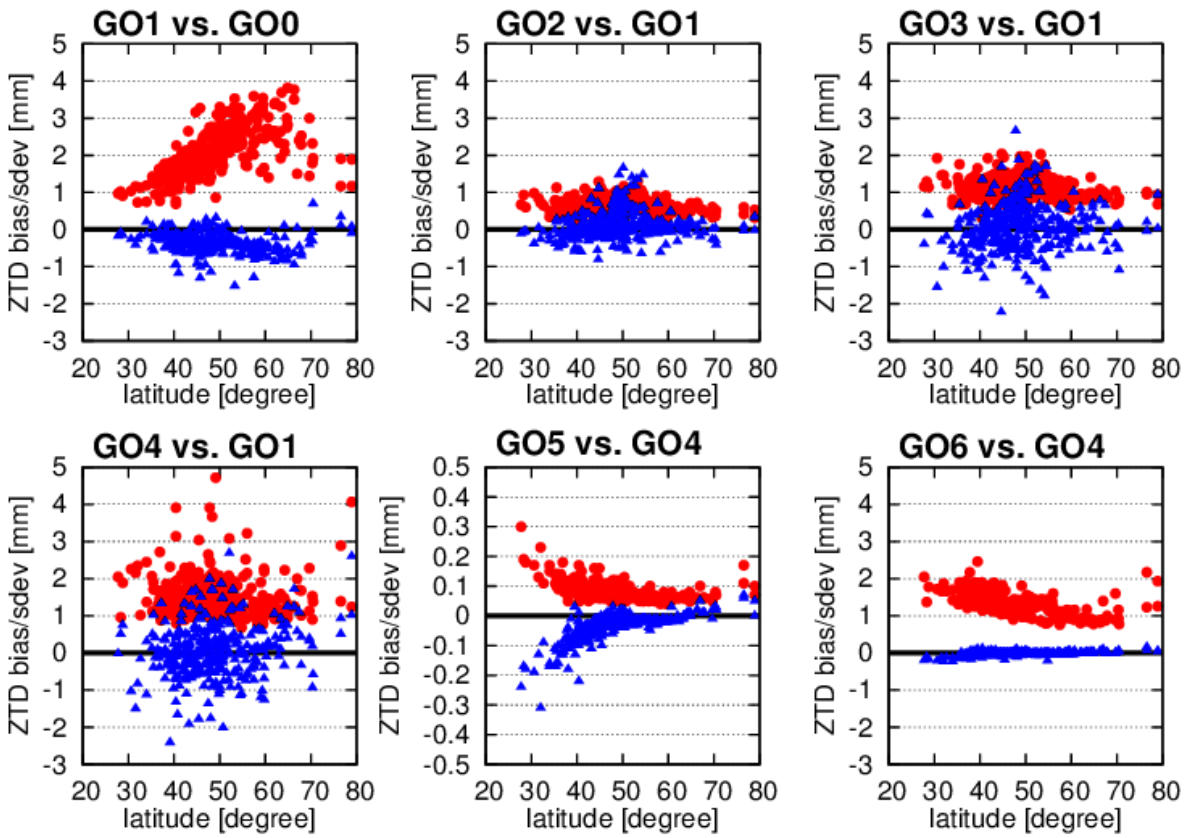

779

780 **Figure 12: Dependence of ZTD biases (blue) and standard deviations (red) from inter-comparisons of GOP 2nd**
781 **reprocessing solution variants on station latitude. Note different y-range for the GO5 vs. GO4 comparison.**

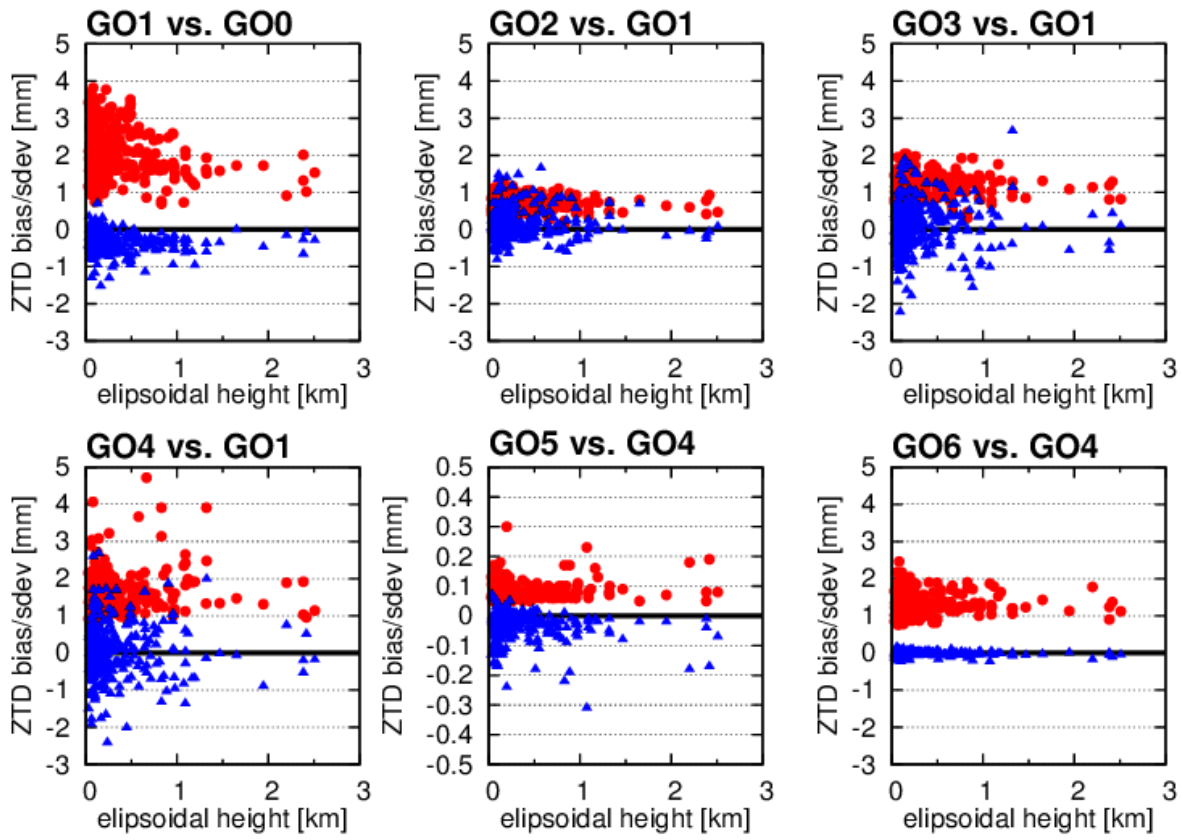

Figure 13: Dependence of ZTD biases (blue) and standard deviations (red) from inter-comparisons of GOP 2nd reprocessing solution variants on station ellipsoidal height. Note different y-range for the GO5 vs. GO4 comparison.

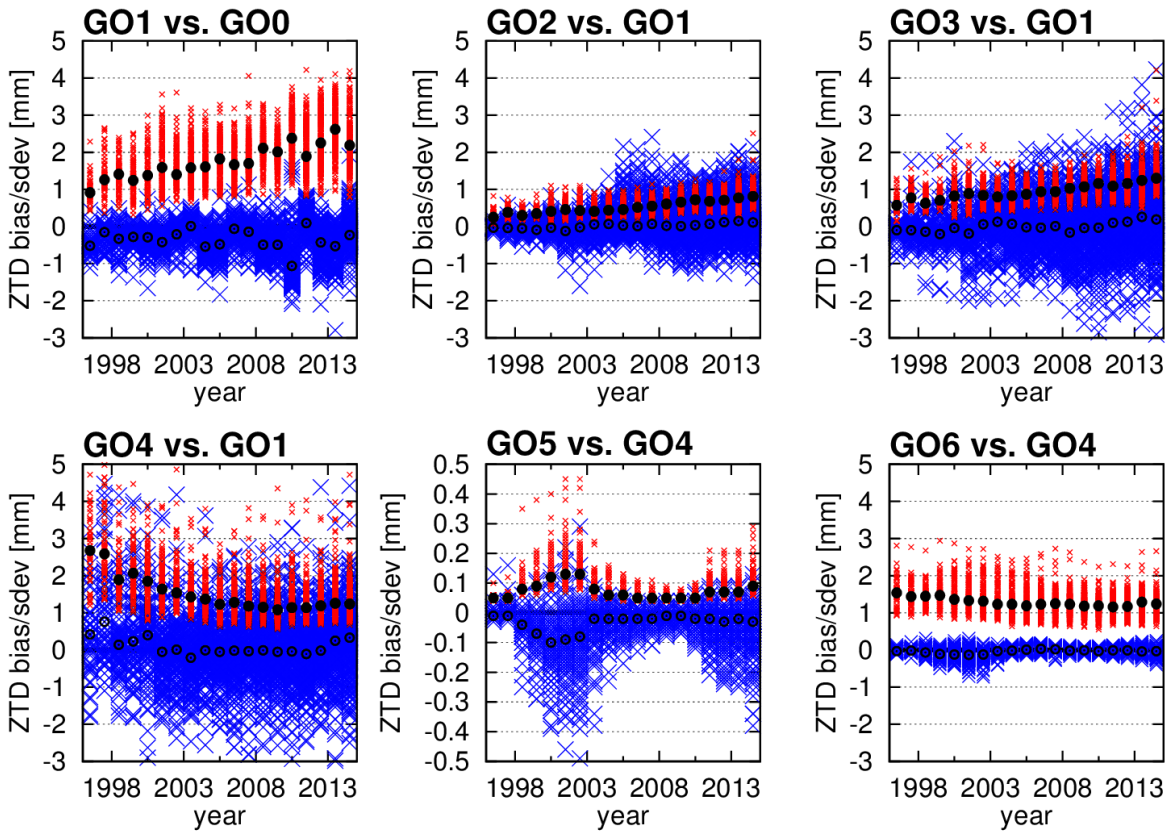

786

787 **Figure 14: Dependence of ZTD biases (blue), mean biases (unfilled black circles), standard deviations (red) and mean**
788 **standard deviations (filled black circles) from inter-comparisons of GOP 2nd reprocessing solution variants on year. Note**
789 **different y-range for the GO5 vs. GO4 comparison.**

790

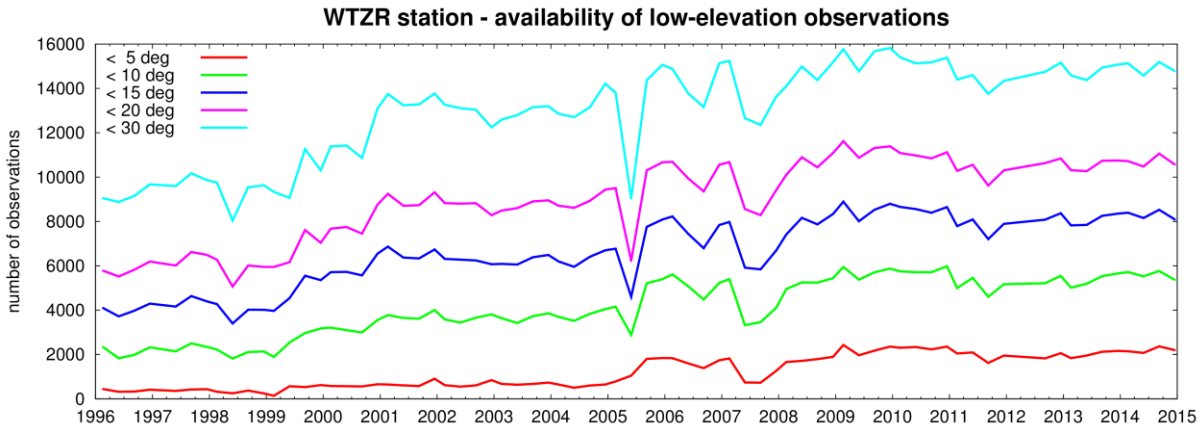

791

792 **Figure 15: Availability of observations at low-elevation angles (below 5°, 10°, 15°, 20° and 30°) for WTZR station.**

793

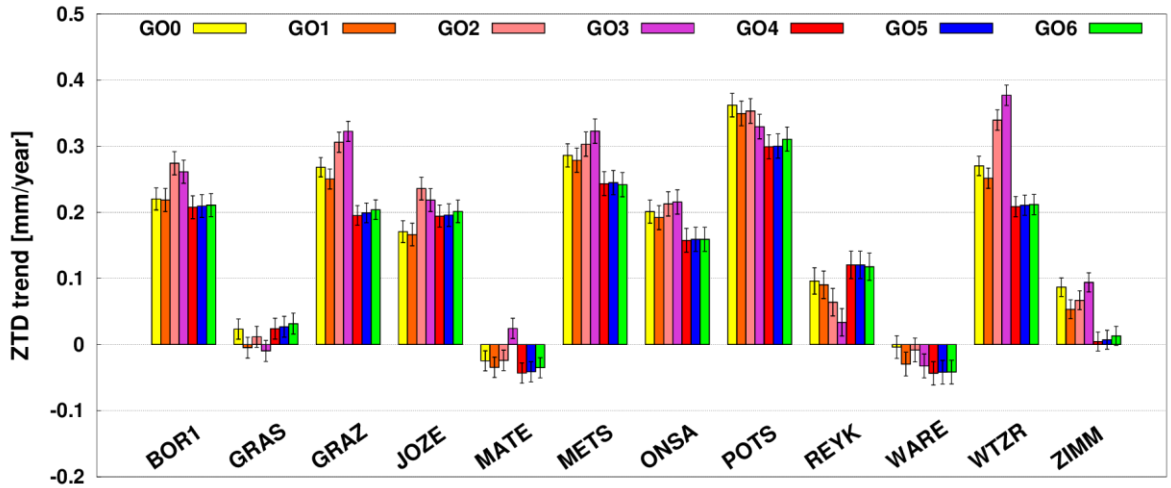

794

795 **Figure 16: Long-term ZTD trend estimates and their formal errors (error bars) for all processing variants**